Disk-Jet Connection in Black Hole Sources

Mayur Bhaskar Shende

Supervisor: Prof. Prasad Subramanian

May 31, 2021

Indian Institute of Science Education and Research (IISER), Pune, India

Observational Motivation

- Interesting observational features about 3C 120, and 3C 111 -

Dips in the X-ray luminosity

Ejections of superluminal radio components from the mm-VLBI core

Observational Motivation

- Interesting observational features about 3C 120, and 3C 111 -

  Dips in the X-ray luminosity

  Ejections of superluminal radio components from the mm-VLBI core

Observational Motivation

- Interesting observational features about 3C 120, and 3C 111 -

Dips in the X-ray luminosity

Ejections of superluminal radio components from the mm-VLBI core

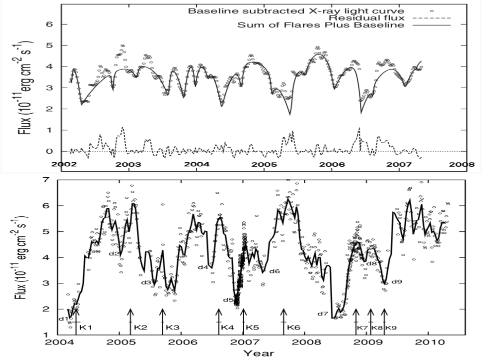

Figure 1: Upper panel: X-ray dips in 3C 120 (Chatterjee et al. 2009), Lower panel: X-ray dips in 3C 111 (Chatterjee et al. 2011)

Observational Motivation

- Interesting observational features about 3C 120, and 3C 111 -

Dips in the X-ray luminosity

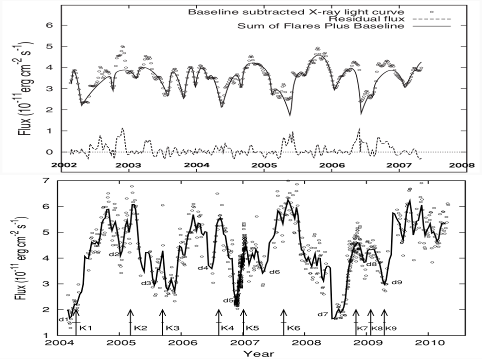

Figure 1: Upper panel: X-ray dips in 3C 120 (Chatterjee et al. 2009), Lower panel: X-ray dips in 3C 111 (Chatterjee et al. 2011)

Ejections of superluminal radio components from the mm-VLBI core

Observational Motivation

- Interesting observational features about 3C 120, and 3C 111 -

Dips in the X-ray luminosity

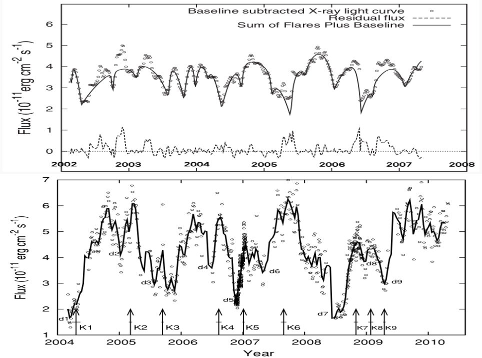

Figure 1: Upper panel: X-ray dips in 3C 120 (Chatterjee et al. 2009), Lower panel: X-ray dips in 3C 111 (Chatterjee et al. 2011)

Ejections of superluminal radio components from the mm-VLBI core

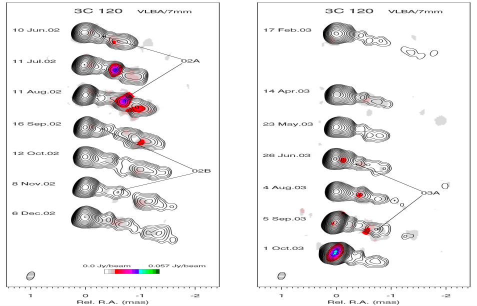

Figure 2: VLBA (43 GHz) images of blobs in 3C 120 (Chatterjee et al. 2009)

Launching of episodic jets from black hole accretion disks

- We draw analogies with Coronal Mass Ejections (CMEs) from the solar corona (Shende et al. 2019, ApJ, 877,130)

Launching of episodic jets from black hole accretion disks

- We draw analogies with Coronal Mass Ejections (CMEs) from the solar corona (Shende et al. 2019, ApJ, 877,130)

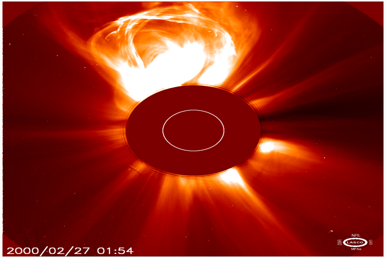

Figure 3: CME (from SOHO/LASCO database)

Launching of episodic jets from black hole accretion disks

- We draw analogies with Coronal Mass Ejections (CMEs) from the solar corona (Shende et al. 2019, ApJ, 877,130)

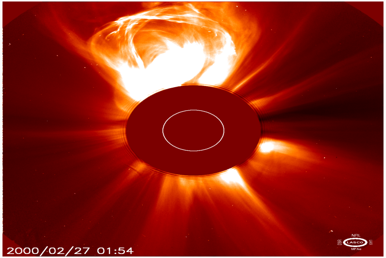

Figure 3: CME (from SOHO/LASCO database)

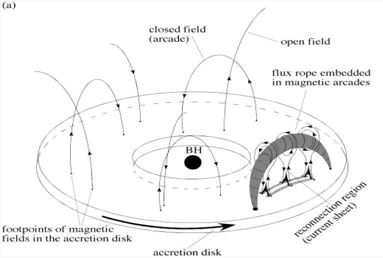

Figure 4: Blob as a flux rope (Yuan et al. 2009)

Launching of episodic jets from black hole accretion disks

- We draw analogies with Coronal Mass Ejections (CMEs) from the solar corona (Shende et al. 2019, ApJ, 877,130)

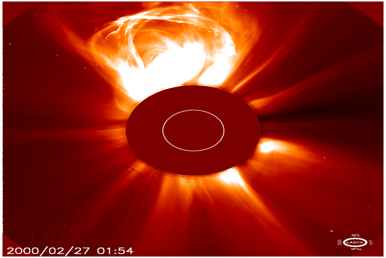

Figure 3: CME (from SOHO/LASCO database)

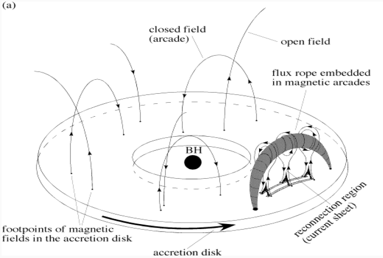

Figure 4: Blob as a flux rope (Yuan et al. 2009)

Toroidal instability of pre-existing flux ropes

Launching of episodic jets from black hole accretion disks

- We draw analogies with Coronal Mass Ejections (CMEs) from the solar corona (Shende et al. 2019, ApJ, 877,130)

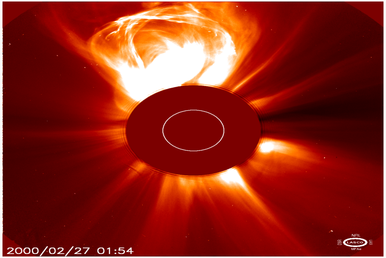

Figure 3: CME (from SOHO/LASCO database)

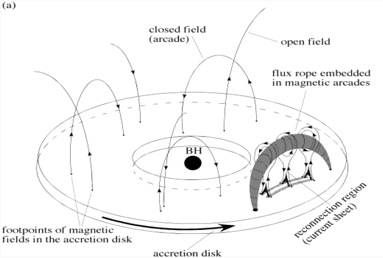

Figure 4: Blob as a flux rope (Yuan et al. 2009)

Toroidal instability of pre-existing flux ropes

Forces acting on a blob = Lorentz self-force + Lorentz force due to external poloidal fields + Gravitational pull

Results and conclusions

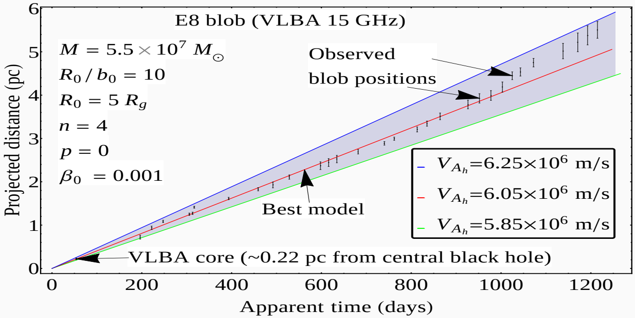

Figure 5: Height–time profile of a representative plasmoid for different values of V_{A_h} compared with observations of blob E8 of 3C 120

Parameter			% change in β_{app}
V_{A_h}	Best fit	6050 km/s	
	% change	-3.31	-12.63
	% change	+2.14	+16.15
β_0	Best fit	0.001	
	% change	-99	-0.02
	% change	+900	+0.1
n	Best fit	4	
	% change	-10	+1.41
	% change	+10	-0.93
R_0	Best fit	5 R_g	
	% change	-0.8	+16.94
	% change	+1	-15.16
R_0/b_0	Best fit	10	
	% change	-4	-12.25
	% change	+4	+16.15

Results and conclusions

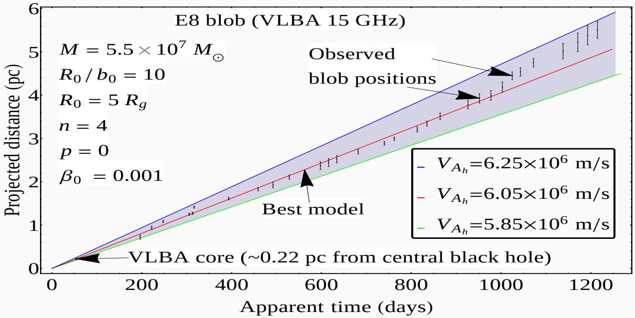

Figure 5: Height–time profile of a representative plasmoid for different values of $V_{\mathrm{A_h}}$ compared with observations of blob E8 of 3C 120

Parameter			% change in β_{app}
$V_{\mathrm{A_h}}$	Best fit	6050 km/s	
	% change	-3.31	-12.63
	% change	+2.14	+16.15
β_0	Best fit	0.001	
	% change	-99	-0.02
	% change	+900	+0.1
n	Best fit	4	
	% change	-10	+1.41
	% change	+10	-0.93
R_0	Best fit	5 R_{g}	
	% change	-0.8	+16.94
	% change	+1	-15.16
R_0/b_0	Best fit	10	
	% change	-4	-12.25
	% change	+4	+16.15

- Model predictions for the time evolution of plasmoids agree well with the observed trajectories

Results and conclusions

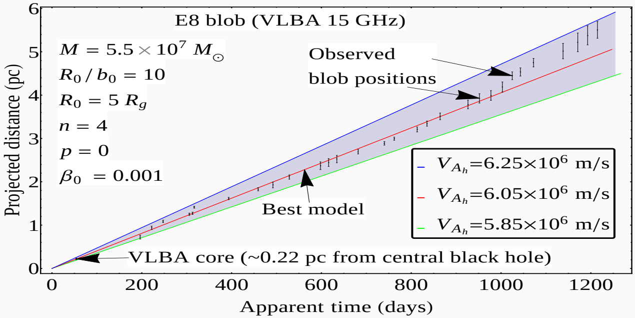

Figure 5: Height–time profile of a representative plasmoid for different values of $V_{\mathrm{A_h}}$ compared with observations of blob E8 of 3C 120

Parameter			% change in β_{app}
$V_{\mathrm{A_h}}$	Best fit	6050 km/s	
	% change	-3.31	-12.63
	% change	+2.14	+16.15
β_0	Best fit	0.001	
	% change	-99	-0.02
	% change	+900	+0.1
n	Best fit	4	
	% change	-10	+1.41
	% change	+10	-0.93
R_0	Best fit	5 R_g	
	% change	-0.8	+16.94
	% change	+1	-15.16
R_0/b_0	Best fit	10	
	% change	-4	-12.25
	% change	+4	+16.15

- Model predictions for the time evolution of plasmoids agree well with the observed trajectories
- We analyze the sensitivity of the model predictions to changes in the model parameters, by way of outlining a viable parameter space

- Interesting observational features about 3C 120, and 3C 111 -

Dips in the X-ray luminosity

Ejections of superluminal radio components from the mm-VLBI core

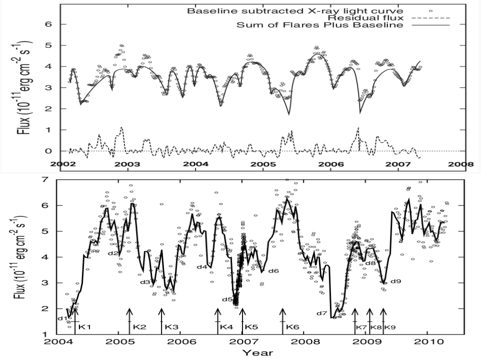

Figure 6: Upper panel: X-ray dips in 3C 120 (Chatterjee et al. 2009), Lower panel: X-ray dips in 3C 111 (Chatterjee et al. 2011)

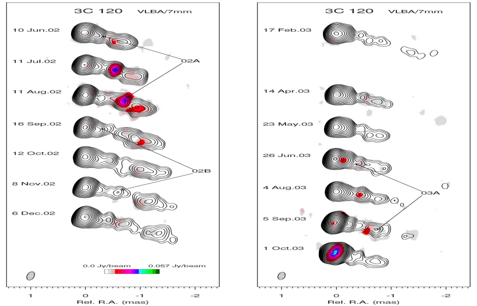

Figure 7: VLBA (43 GHz) images of blobs in 3C 120 (Chatterjee et al. 2009)

Viscous infalling timescales of inner accretion disks

- X-ray dip durations: 3C 120: 5-120 days, 3C 111: 73-402 days, GRS 1915+105: 5-6 s

Viscous infalling timescales of inner accretion disks

- X-ray dip durations: 3C 120: 5-120 days, 3C 111: 73-402 days, GRS 1915+105: 5-6 s
- Suggests that accretion disk corona is periodically "emptied" and "refilled"

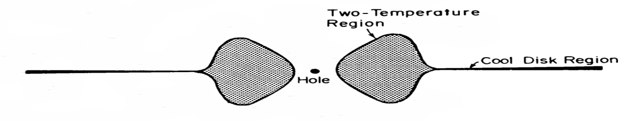

Viscous infalling timescales of inner accretion disks

- X-ray dip durations: 3C 120: 5-120 days, 3C 111: 73-402 days, GRS 1915+105: 5-6 s
- Suggests that accretion disk corona is periodically "emptied" and "refilled"

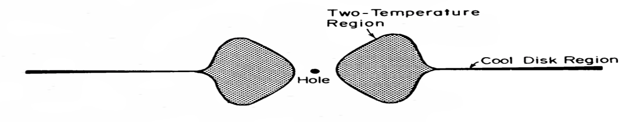

- We address these timescales as viscous infalling timescale in our model (Shende et al. 2021, MNRAS, 501, 3741)

Viscous infalling timescales of inner accretion disks

- X-ray dip durations: 3C 120: 5-120 days, 3C 111: 73-402 days, GRS 1915+105: 5-6 s
- Suggests that accretion disk corona is periodically "emptied" and "refilled"

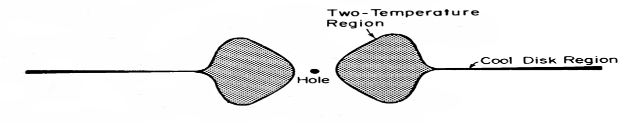

- We address these timescales as viscous infalling timescale in our model (Shende et al. 2021, MNRAS, 501, 3741)
- Physical prescription for viscosity instead of specifying the values of α

Viscous infalling timescales of inner accretion disks

- X-ray dip durations: 3C 120: 5-120 days, 3C 111: 73-402 days, GRS 1915+105: 5-6 s
- Suggests that accretion disk corona is periodically "emptied" and "refilled"

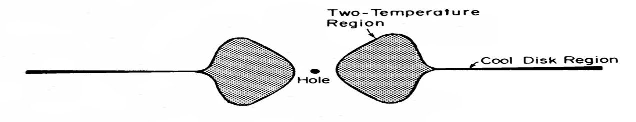

- We address these timescales as viscous infalling timescale in our model (Shende et al. 2021, MNRAS, 501, 3741)
- Physical prescription for viscosity instead of specifying the values of α
- Using published simulation results for cosmic ray diffusion through turbulent magnetic fields

Results and conclusions

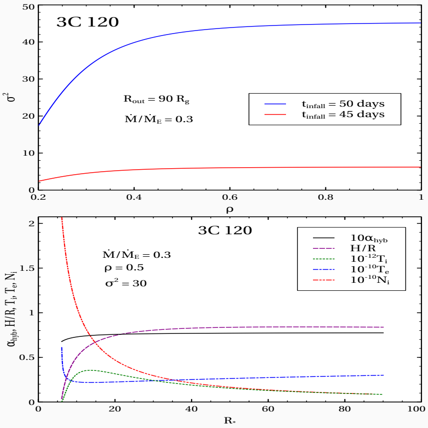

Figure 8: Upper panel: Parameter space corresponding to X-ray dip in the range 45–50 days in 3C 120, lower panel: Representative accretion disk models for 3C 120

Parameter	% change in reference	% change in in $t_{\rm infall}$
ρ	+10	-0.1
	-10	+0.1
σ^2	+10	+0.5
	-10	-0.5
$R_{\rm out}$	+10	+15
	-10	-15

Table 1: Sensitivity analysis of parameters with $\rho_{\rm ref} = 0.5$, $\sigma^2_{\rm ref} = 10$, $R_{\rm out_{ref}} = 90\ R_{\rm g}$: fiducial model for 3C 120

Results and conclusions

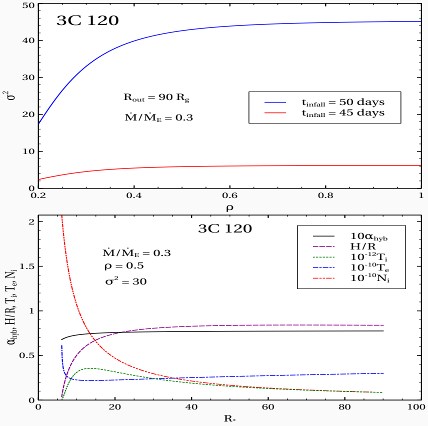

Figure 8: Upper panel: Parameter space corresponding to X-ray dip in the range 45–50 days in 3C 120, lower panel: Representative accretion disk models for 3C 120

Parameter	% change in reference	% change in in $t_{\rm infall}$
ρ	+10	-0.1
	-10	+0.1
σ^2	+10	+0.5
	-10	-0.5
$R_{\rm out}$	+10	+15
	-10	-15

Table 1: Sensitivity analysis of parameters with $\rho_{\rm ref} = 0.5$, $\sigma^2_{\rm ref} = 10$, $R_{\rm out_{ref}} = 90\ R_g$: fiducial model for 3C 120

Conclusions:

Results and conclusions

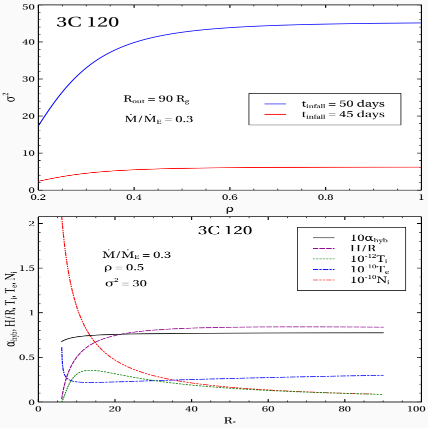

Figure 8: Upper panel: Parameter space corresponding to X-ray dip in the range 45–50 days in 3C 120, lower panel: Representative accretion disk models for 3C 120

Parameter	% change in reference	% change in t_{infall}
ρ	+10	-0.1
	-10	+0.1
σ^2	+10	+0.5
	-10	-0.5
R_{out}	+10	+15
	-10	-15

Table 1: Sensitivity analysis of parameters with $\rho_{\text{ref}} = 0.5$, $\sigma^2_{\text{ref}} = 10$, $R_{\text{out}_{\text{ref}}} = 90\ R_g$: fiducial model for 3C 120

Conclusions:

- Instead of specifying the values of α, we give the physical prescription for viscosity in the hot, inner disk

Results and conclusions

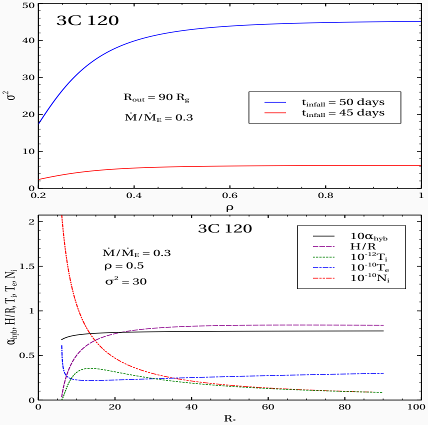

Figure 8: Upper panel: Parameter space corresponding to X-ray dip in the range 45–50 days in 3C 120, lower panel: Representative accretion disk models for 3C 120

Parameter	% change in reference	% change in t_{infall}
ρ	+10	-0.1
	-10	+0.1
σ^2	+10	+0.5
	-10	-0.5
R_{out}	+10	+15
	-10	-15

Table 1: Sensitivity analysis of parameters with $\rho_{ref} = 0.5$, $\sigma^2_{ref} = 10$, $R_{out_{ref}} = 90\ R_g$: fiducial model for 3C 120

Conclusions:

- Instead of specifying the values of α, we give the physical prescription for viscosity in the hot, inner disk
- The disk infall time-scales (t_{infall}) obtained with this model are in good agreement with X-ray observations of 3C 120, 3C 111 and GRS 1915+105

Conclusions and current work

Broad conclusion:

- Our work outlines a plausible scenario for episodes of (inner) disk collapse accompanied by blob ejection

Current work:

- Origin of (matter dominated) steady winds from accretion disk coronae

(1) Self-consistent inflow-outflow solutions: fluid description
(2) Particle acceleration mechanisms in the disk corona: particle description

- We aim to bridge this gap and show how the high energy tail of the accelerated particle population is preferentially launched outwards to form a relativistic wind (Shende et al. 2021 in preparation)

Conclusions and current work

Broad conclusion:

- Our work outlines a plausible scenario for episodes of (inner) disk collapse accompanied by blob ejection

Current work:

- Origin of (matter dominated) steady winds from accretion disk coronae

(1) Self-consistent inflow-outflow solutions: fluid description

(2) Particle acceleration mechanisms in the disk corona: particle description

- We aim to bridge this gap and show how the high energy tail of the accelerated particle population is preferentially launched outwards to form a relativistic wind (Shende et al. 2021 in preparation)

Conclusions and current work

Broad conclusion:

- Our work outlines a plausible scenario for episodes of (inner) disk collapse accompanied by blob ejection

Current work:

- Origin of (matter dominated) steady winds from accretion disk coronae

(1) Self-consistent inflow-outflow solutions: fluid description

(2) Particle acceleration mechanisms in the disk corona: particle description

- We aim to bridge this gap and show how the high energy tail of the accelerated particle population is preferentially launched outwards to form a relativistic wind (Shende et al. 2021 in preparation)

Conclusions and current work

Broad conclusion:

- Our work outlines a plausible scenario for episodes of (inner) disk collapse accompanied by blob ejection

Current work:

- Origin of (matter dominated) steady winds from accretion disk coronae

(1) Self-consistent inflow-outflow solutions: fluid description
(2) Particle acceleration mechanisms in the disk corona: particle description

- We aim to bridge this gap and show how the high energy tail of the accelerated particle population is preferentially launched outwards to form a relativistic wind (Shende et al. 2021 in preparation)

Conclusions and current work

Broad conclusion:

- Our work outlines a plausible scenario for episodes of (inner) disk collapse accompanied by blob ejection

Current work:

- Origin of (matter dominated) steady winds from accretion disk coronae

(1) Self-consistent inflow-outflow solutions: fluid description
(2) Particle acceleration mechanisms in the disk corona: particle description

- We aim to bridge this gap and show how the high energy tail of the accelerated particle population is preferentially launched outwards to form a relativistic wind (Shende et al. 2021 in preparation)

Thank You!